GeoHazards

MDPI

Review

Seismo-Stratigraphic Data of the Gulf of Pozzuoli (Southern Tyrrhenian Sea, Italy): A Review and Their Relationships with the New Bradyseismic Crisis

Gemma Aiello

Istituto di Scienze Marine (ISMAR), Consiglio Nazionale delle Ricerche (CNR), Sezione Secondaria di Napoli, 80133 Napoli, Italy; gemma.aiello@cnr.it

Abstract

Seismo-stratigraphic data of the Gulf of Pozzuoli have been revised with the aim of identifying the tectonic structures controlling the area in more detail and to highlight the possible relationships of the morpho-structures with the new bradyseismic crisis, still in course. In particular, the relationships between the tectonic structures, consisting of both normal faults and folds, and the possible rising of fluids have been analyzed based on seismic interpretation. We hypothesize that the normal faults occurring in this area have possibly controlled the rising of fluids in these extensional structures. The fluid uprising could possibly be related to the increasing gas activity of the Solfatara–Pisciarelli area onshore during the active bradyseismic crisis (2024–2025). The proposed mechanism is controlled by the occurrence of a heat source, possibly a magmatic reservoir, in the continental crust and/or the mantle, genetically related to the presence of submerged hydrothermal discharges in the coastal areas of the Campania region. To achieve this objective, detailed seismo-stratigraphic sections of the Gulf of Pozzuoli have been constructed, focusing on the areas characterized by tectonic activity. Fluid uprising is mainly controlled by the tectonic setting of the Gulf of Pozzuoli, characterized by anticlines and synclines, representing important structural and stratigraphic traps.

Keywords: seismo-stratigraphic units; Gulf of Pozzuoli; tectonic structures; bradyseismic crisis; fluid uprising

Received: 15 July 2025
Revised: 11 August 2025
Accepted: 13 August 2025
Published: 15 August 2025

Citation: Aiello, G. Seismo-Stratigraphic Data of the Gulf of Pozzuoli (Southern Tyrrhenian Sea, Italy): A Review and Their Relationships with the New Bradyseismic Crisis. *GeoHazards* **2025**, *6*, 46. https://doi.org/10.3390/geohazards6030046

1. Introduction

The problem of fluid and gas uprising on seismic sections based on literature data has been studied in depth, since gas identification on seismic sections is an important task. Because it offers a quick way to identify and map gas accumulations, reflection seismics is a crucial instrument for shallow gas investigations [1–21]. The best research areas for these are the Campi Flegrei buried caldera, the Naples Bay, including Ischia Island, and the Solfatara–Pisciarelli geothermal zone [4,5,7,22]. The Matese Mountains are among the regions of the Southern Apennines that are of great significance from a geothermal and geochemical perspective. Important impregnations of gas have also been detected at the Volturno river mouth [12,23] and in the Cilento offshore [16]. Moreover, a close relationship exists between shallow gas occurrence, creeping processes, and high sedimentary supply at the Volturno and Sarno river mouths [24].

On the Navarian continental margin, the seismic sections and the geochemical data display the occurrence of hydrocarbon gas at shallow water depths [1]. These hydrocarbons

and gases are associated with three main types of acoustic anomalies, which prevail in the northern portion of the basin. On the seismic records of the continental slope, the acoustic variations are frequently linked to gas hydrates and diagenetic limits.

A basic paper on the detection of shallow gas in marine sediments based on the analysis of the seismic sections is that of Judd and Hovland [2]. The main seismic evidence includes acoustic turbidity, enhanced reflections, columnar disturbances or gas chimneys, and acoustic blanking. Acoustic turbidity is characterized by chaotic reflections, controlled by the scattering of acoustic energy, and is often associated with a pull-down of seismic reflections in the presence of gas. A portion of amplified (enhanced) reflections are reflected by coherent seismic reflections with an increased amplitude, which can indicate the lateral extension of acoustic turbidity zones. While the enhanced reflections are associated with silty, sandy, and porous deposits, acoustic turbidity is characteristic of fine-grained sediments, rich in clays. Hovland and Judd [25] have identified gas chimneys as vertical features where the upwards migration of pore fluids has destroyed the normal sequence of seismic reflectors. Moreover, bright spots have often been detected on Sparker seismic sections [2].

One of the most important acoustic anomalies associated with the occurrence of gas is represented by acoustic blanking, where patches lacking seismic reflectors are in coincidence with an inferred gas record. This can be managed by either the absorption of acoustic energy in the surrounding sediments, which are charged with gas, or by the disruption of sediment layers due to the migration of pore fluids, including the gas [2]. The geochemical signatures include petroleum drilling and mud analysis, seabed sediment analysis, and sea water sampling.

The seabed surface features associated with the occurrence of gas are pockmarks, seabed domes, and mud diapirs. Pockmarks are depressions of the seafloor, which are controlled by the removal of sediments by the escaping fluids. They are widespread on the Italian continental margins [21], from shallow water depths (Adriatic Sea, Strait of Sicily) to deep-sea sectors at active continental margins (Ionian Sea) and passive continental margins (Tyrrhenian Sea). Based on the systematic study of Spatola et al. [21], 93% of pockmarks are concentrated at water depths less than 800 m and mainly on flat and gently sloping seafloors, and they also depend on lithology, being concentrated in muddy sands and sands.

Active seabed domes in the Naples Bay have been discussed [11], focusing on the Banco della Montagna seabed dome. Less extensive NW-SE alignments are found in the Banco della Montagna core sector, but the spatial density of the cones and pockmarks indicates the main NE-SW alignments defining the northeastern and southern boundaries of the dome. Using ROV observations on the seafloor and echo-sounder images of the water column, 37 gas emissions have been identified in this region and explained according to a mechanism of submarine hydrothermal gas manifestations [11].

Mud diapirs, consisting of shale diapirs or clay diapirs, are controlled by the subsurface overpressure, have a tectonic, diagenetic, or sedimentary origin, and form as a consequence of underconsolidation in sediments characterized by low permeability. Among others, Carfagna et al. [19] have shown the occurrence of mud diapirs and mud volcanoes in Nirano, located in Northern Italy, while Brindisi et al. [20] have used passive seismic measurements to characterize the gas reservoirs located in mud volcanoes of Northern Italy.

One aim of this paper is to assess the occurrence of gas in the Gulf of Pozzuoli based on seismo-stratigraphic data, previously collected in the Gulf of Pozzuoli in the frame of the CARG project (Figure 1) [26]. Another aim is to revise the seismo-stratigraphic data, previously interpreted [26,27], to obtain an updated geological interpretation.

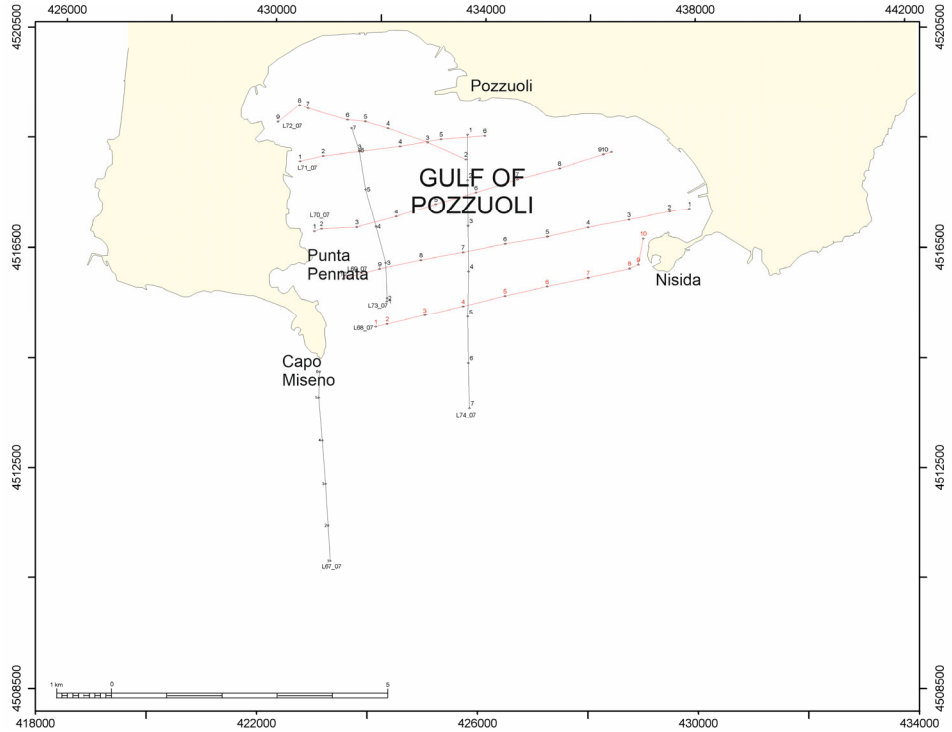

Figure 1. Location map of the Sparker profiles analyzed in this paper (Gulf of Pozzuoli). Tie seismic sections (parallel to the shoreline, red lines): L72_7, L71_7, L70_7, L69_7, L68_7. Dip seismic sections (perpendicular to the shoreline, black lines): L68_7, L67_7, L74_7. Numbers 1 to 10 in the picture represent the shot points on the seismic lines.

Shallow gas represents a significant marine geohazard [28], together with earthquakes, volcanism, tsunamis, submarine mass movements, fluid flows through marine sediments, cascading, and other significant geological processes [28]. A fluid discharge from the bottom could be a geohazard to drilling operations or seafloor infrastructure directly, or it could be a geohazard to vessels, rigs, and floating equipment above by causing a loss of buoyancy and density [28].

As a general rule, in the Naples Bay and in particular, in the Gulf of Pozzuoli, shallow gas marine geohazards could represent a primary marine and geological hazard. In the Gulf of Pozzuoli, tectonic control is prevalent in the eustatic area: here, uplifted seafloor areas, normal faults genetically related to the apex of the resurgent dome of the caldera structure, and multiple fluid venting sites occur during the post-caldera phase of activity of the Phlegrean volcanic complex.

Offshore, in the Naples harbor mounded morphologies, the uprising, pressurization, and release of He and CO_2 from mantle melts and decarbonation reactions of crustal rocks have been recorded. The presence of a mantle source mixed with crustal fluids beneath the Gulf of Naples is suggested by the likelihood that these gases are comparable to those that fuel the hydrothermal systems of the active volcanoes of Ischia, Campi Flegrei, and Somma-Vesuvius. Non-volcanic disturbances that may precede undersea eruptions and/or hydrothermal explosions include seabed doming, faulting, and gas discharge and are genetically related to the caldera unrest.

While our previous papers in this area mainly focused on the distribution of the seismo-stratigraphic units in the Gulf of Pozzuoli (here, fourteen seismo-stratigraphic units have been detected, both volcanic and sedimentary) [26,27], in this paper, we reassess the Sparker seismic sections to highlight the occurrence of gas and the possible relationships with the present-day bradyseismic crisis. In fact, the structures previously interpreted as volcanic dykes [26], genetically related to extensional structures, are herein interpreted as possible

gas impregnations, possibly related to the massive gas emissions at the Solfatara and Pisciarelli craters during the present-day bradyseismic crisis. In this framework, we hypothesize that the Solfatara–Pisciarelli geothermal system [7,29–33] could be genetically related to the gas emissions identified in the Gulf of Pozzuoli based on seismo-stratigraphic analysis.

2. Earthquakes and Bradyseism

Risky volcanoes that have recently seen seismic activity include Vesuvius, Campi Flegrei, Ischia, and Procida. The Campi Flegrei bradyseism has been primarily responsible for the recent earthquakes. At least 10 million years have passed since the caldera's last eruption. Seismicity, ground deformations, and volcanism are thought to be connected to the reactivation of the Campi Flegrei caldera. The volcanic structures predominate in the raised portion of the caldera, causing both short-term deformations, or bradyseism, and long-term deformation, or resurgence. From 1969 to 1972 and 1982 to 1984, there were two major bradyseismic crises.

During recent years, significant earthquakes have occurred in Campi Flegrei and Naples Bay (Table 1; https://terremoti.ingv.it/events, accessed on 27 June 2025). The earthquakes represent a main marine geohazard in the Naples area [24,34–39].

In 2023, 572 earthquakes occurred at Campi Flegrei and Vesuvius, based on the INGV catalog. The most significant ones (magnitude between 3 and 4) are reported in Table 1.

Bradyseism and Campi Flegrei earthquakes are genetically connected. A 4.3-magnitude earthquake hit Campi Flegrei on 27 September 2023 (Table 1). For a few weeks, it was a part of a seismic sequence involving Campi Flegrei and was the longest-lasting earthquake to strike the area in forty years. To understand this seismological record, Kilburn et al. [40] constructed a seismological model based on the evolution from an elastic state to an inelastic one. In this model, the rocks fracture more and more, and the breaking originates beneath the faults. In this framework, the frequency of local earthquakes is genetically related to the rate of ground deformation, as happens in bradyseismic crises. A few earthquakes are caused by ground deformation in the early stages, but as crustal stress grows, the same amount of ground deformation eventually accelerates earthquake frequency. The published findings provided information for predicting whether the volcano will erupt or subside before the volcanic eruption, depending on how much the caldera unrest has affected the crust's geometry.

Another important earthquake involved Campi Flegrei on 13 March 2025 (Table 1). In this framework, Giudicepietro et al. [41] suggested a burst model to explain the present-day volcanic and seismic crisis. The volcanic area of Campi Flegrei is going through a long period of gradual intensification of activity that began in 2005. During this period, an increase in general seismicity, an intensification of gas emissions, and an acceleration of ground deformation have been observed. The zone of maximum deformation coincides with the central part of the caldera, which has risen by about 140 cm since 2005. The amount of uplift gradually decreases from the center of the caldera outwards, giving the deformation field a general bell shape.

Volcanic–tectonic seismic sequences, characterized by very short time intervals between one seismic event and another one, which have become increasingly frequent since the beginning of 2021, have been identified [41]. Peculiar seismic swarms known in the literature as "burst-like swarms" have been recognized among these sequences. These sequences, also known as "burst swarms", are characterized by such short intervals between one event and another that the individual earthquakes are often difficult to recognize in the seismogram [41].

Table 1. Significant earthquakes in the Bay of Naples until March 2025 (https://terremoti.ingv.it/events, accessed on 9 June 2025).

Time	Magnitude (MW)	Location	Depth	Latitude	Longitude
27 September 2023	4.2	Campi Flegrei	3 km	40°82′	14°16′
2 October 2023	4.0	Campi Flegrei	3 km	40°83′	14°15′
7 September 2023	3.8	Campi Flegrei	3 km	40°83′	14°15′
16 October 2023	3.6	Campi Flegrei	2 km	40°8′	14°14′
11 June 2023	3.6	Campi Flegrei	3 km	40° 83′	14°11′
18 August 2023	3.6	Campi Flegrei	2 km	40°83′	14°14′
23 November 2023	3.1	Campi Flegrei	3 km	40°83′	14°14′
17 February 2024	3.0	Campi Flegrei	3 km	40°84′	14°12′
3 March 2024	3.4	Campi Flegrei	3 km	40°82′	14°16′
11 March 2024	3.0	Vesuvius	3 km	40°85′	14°.40′
14 April 2024	3.7	Campi Flegrei	2 km	40°83′	14°14′
14 April 2024	2.1	Vesuvius	8 km	40°81′	14°35′
27 April 2024	3.9	Campi Flegrei	3 km	40°81′	14°09′
28 April 2024	3.1	Vesuvius	0 km	40°82′	14°83′
10 May 2025	3.7	Campi Flegrei	3 km	40°80′	14°11′
20 May 2024	3.9	Campi Flegrei	3 km	40°83′	14°14′
8 June 2024	3.7	Campi Flegrei	3 km	40°83′	14°15′
2 July 2024	3.9	Campi Flegrei	3 km	40°81′	14°16′
18 July 2024	3.6	Campi Flegrei	2 km	40°83′	14°15′
30 August 2024	3.7	Campi Flegrei	2 km	40°83′	14°15′
22 September 2024	2.2	Vesuvius	2 km	40°82′	14°83′
13 October 2024	2.6	Campi Flegrei	2 km	40°83′	14°15′
9 November 2024	2.8	Vesuvius	1 km	40°81′	14°82′
6 December 2024	2.7	Campi Flegrei	0 km	40°82′	14°14′
17 January 2025	3.0	Campi Flegrei	2 km	40°83′	14°13′
28 January 2025	2.6	Vesuvius	1 km	40°82′	14°43′
5 February 2025	3.1	Campi Flegrei	3 km	40°83′	14°15′
9 February 2025	2.5	Vesuvius	1 km	40°82′	14°43′
17 February 2025	3.9	Campi Flegrei	2 km	40°83′	14°15′
17 February 2025 (among others)	2.7	Campi Flegrei	2 km	40°83′	14°15′
18 February 2025	3.1	Campi Flegrei	1 km	40°83′	14°14′
7 March 2025	3.2	Campi Flegrei	1 km	40°82′	14°13′
13 March 2025	4.6	Campi Flegrei	2 km	40°82′	14°16′

The present-day bradyseismic crisis can be compared with the old ones. Instances of gradual vertical ground movement (bradyseism) have been recorded since ancient Roman times. Since the 1800s, vertical ground shifts have been noted, as evidenced by the sea level markings found on the remains of a Roman market ("Serapeo") in Pozzuoli, indicating a slow sinking of the region [42–45].

Thorough ground surveying conducted in the region revealed that the highest level of subsidence occurred in the municipality of Pozzuoli, gradually diminishing towards the east and the west [46]. The ground's elevation continued to drop until 1968, at which point a method that links the tracking of ground deformation with building behavior was established to assess the degree of increasing damage caused by bradyseism to typical Phlegrean buildings in near-real time. The adopted models (hazard, exposure, and vulnerability) have been described.

Two primary events of soil elevation affecting the Pozzuoli region during the time intervals of 1970–1972 and 1982–1984 have contributed to the uplift, measured against the earlier levels, which were 170 cm and 182 cm at the locations of greatest deformation [46]. The shape of the uplift was contrary to that of the subsidence noted since 1968, with a peak focused on the city of Pozzuoli, and a consistent reduction in the deformation towards the edges of the caldera [46].

Another method of bradyseismic analysis involves the reconstruction of vertical movements through the analysis of the ancient coastal ruins of the Serapis Roman marketplace [44,45]. Three marble columns at Serapis displayed signs of having been submerged at least 7 m, then raised by a similar height. According to the elevation of other coastal ruins in proximity to Serapis, the maximum recorded subsidence at Serapis is 12–17 m [44]. Two uplift periods have been identified, the first occurring a few decades prior to the 1538 eruption in the Phlegrean Fields and the second occurring in two separate episodes, the initial one from 1969 to 1972 and the latter one from 1982 to 1984 [46]. Subsequently, radiocarbon-dated biological indicators on the columns of the Roman market have indicated three 7 m highstands of relative sea level, occurring during the fifth century, the early Middle Ages, and just before the 1538 eruption at Monte Nuovo [45]. The assessment of volcanic hazards is significantly impacted by these cycles of uplift and subsidence, which do not necessarily correspond with volcanic activity (Figure 2).

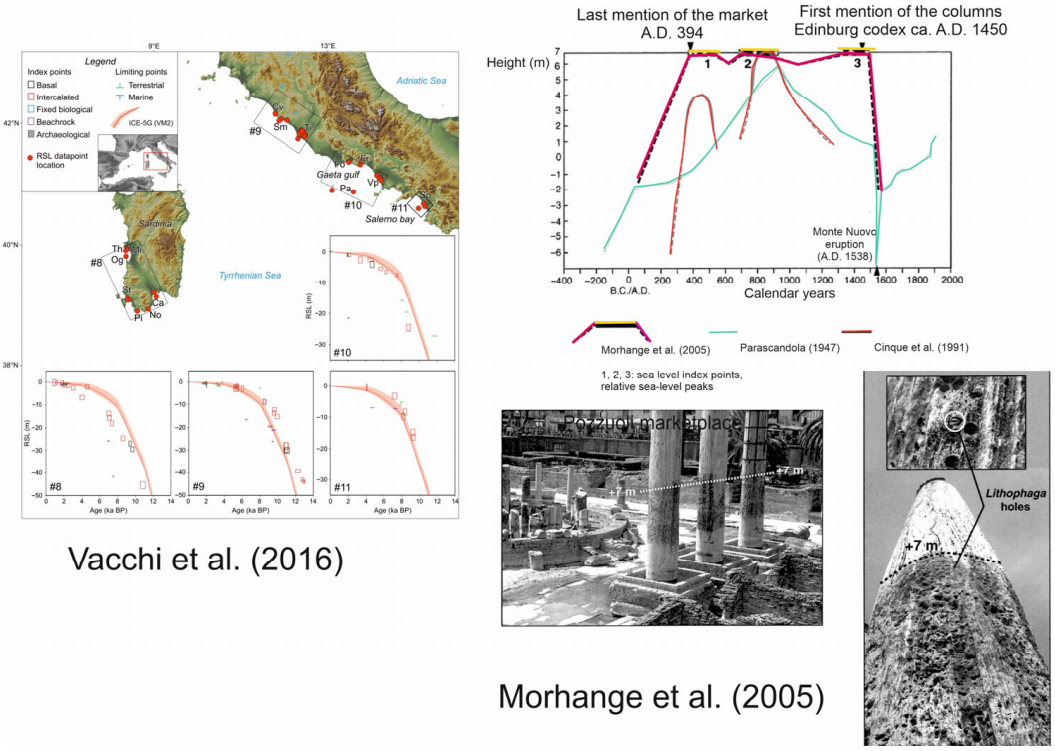

Figure 2. Sea level changes and bradyseismic cycles, adapted from Vacchi et al. [47] and Morhange et al. [45], respectively. On the left, Vacchi et al. [47] have summarized the relative sea level reconstructions at several sites of Southern Italy, including southwestern Sardinia (#8), north–central Latium (#9), the Gulf

of Gaeta (#10) and the Salerno Bay (#11). The approximate locations of the relative sea level data points are represented as red dots. Key: Th, Tharros; Mi, Is Mistras; Or, Gulf of Oristano; Pi, Piscinni Bay and Malfatano Cape; St, Sant'Antioco; Ca, Cagliari; No, Nora; Cv, Civitavecchia; Sm, Santa Marinella; Ti, Tiber Delta; Fo, Fondi coastal plain; Fr, Formia; Po, Pontine Archipelago; Vp, Volturno coastal plain; Sp, Sele coastal plain. On the right, the data of Morhange et al. [45] have been reported. These data regard the Pozzuoli marketplace ("Serapeo") and the construction of a new relative sea level curve, as compared with previous curves, adapted from Parascandola [42] and Cinque et al. [43].

The use of advanced techniques, including geodesy, numerical simulations, and petrology, has allowed us to map the volcanic movements within the caldera over a 16-year period (2007–2023), that is, from the beginning of the new bradyseismic phase of the volcano which is still active [48]. This study suggests that the primary driver of volcanic–tectonic activity is magma rising to depths of less than 8 km, with a gradual and continuous ground uplift that has reached about 1.3 m in the Rione Terra of Pozzuoli between 2006 and the present [48]. Over time, the depth of the deformation source has decreased from roughly 6 km to about 4 km, becoming increasingly shallow. The rising of magma and gas from the primary accumulation area, which is 8 km deep, to lower depths is the cause of this source. Furthermore, the rise of magma and magmatic gases has contributed to the intensification of seismic activity and to the increase in gas emission phenomena, particularly in the Solfatara area. The vertical cumulated displacements have been obtained by combining InSAR ENVISAT (2007–2011) and COSMO-SkyMed data (2011–2023; Figure 3) [48].

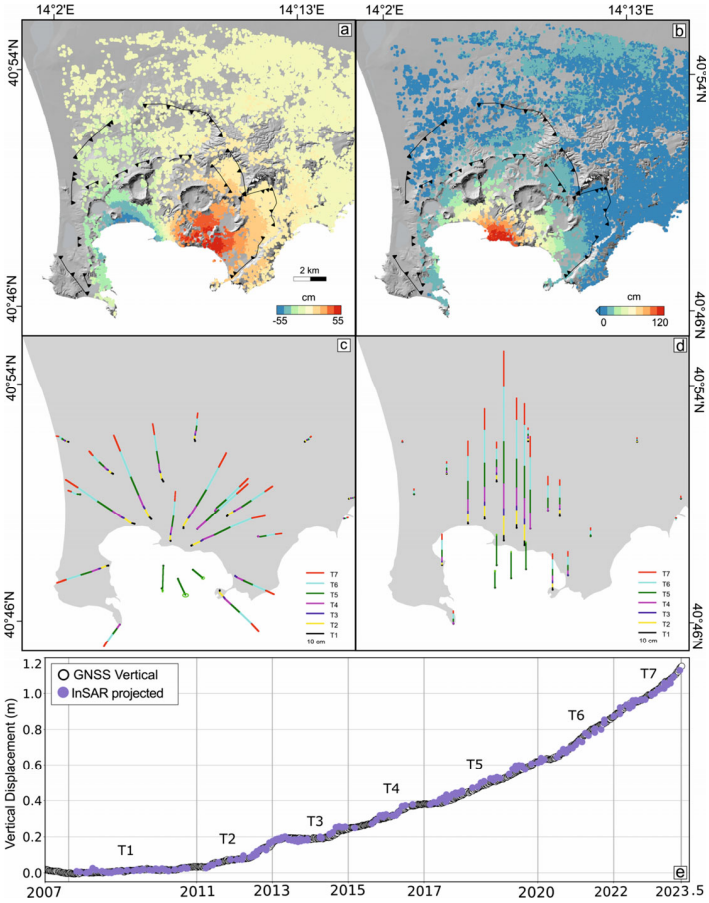

Figure 3. (**a**,**b**) Vertical cumulated displacements obtained by combining InSAR ENVISAT (2007–2011) and COSMO-SkyMed data (2011–2023), respectively. (**c**,**d**) Horizontal and vertical GNSS cumulated displacements, respectively, separated into seven time periods during 2007–2023. (**e**) Vertical displacement time series measured at RITE (black dots) and projected vertical time series from ENVISAT and COSMO-SkyMed datasets (modified after Astort et al.) [48].

Patanè et al. [49] have discussed the seismic images of the pressurized sources and the migration of fluids during the tectonic uplift of the Campi Flegrei caldera in the timespan from 2020 to 2024. After the subsidence period that followed the 1982–1984 bradyseismic crisis, a slow-paced ground uplift at Campi Flegrei caldera began in 2005. Since 2018, the frequency and intensity of volcanic–tectonic earthquakes have progressively increased, with a noticeable increase since 2023 [49]. A new tomographic investigation with data gathered between 2020 and June 2024 was carried out. Three-dimensional velocity models offered higher-resolution pictures of the structure of the central caldera down to about 4 km depth, in contrast to earlier tomographic investigations. The geophysical inversions of the two datasets collected in 2020–2022, characterized by moderate seismicity, and 2023–2024, characterized by severe seismicity, have revealed significant velocity differences across these time periods, ranging from 5% to 10%. These 2023–2024 fluctuations suggest two pressured sources at various depths. The first, situated 3.0–4.0 km below Pozzuoli and offshore, could be a deposit of pressured, high-density fluids or a magma intrusion enriched in supercritical fluids; this conclusion is consistent with current ground deformation research and estimated source depths. Furthermore, a secondary, shallower pressurized source was created at a depth of about 2.0 km beneath the Solfatara–Pisciarelli region because of the upward movement of magmatic fluids interacting with the geothermal system.

3. Geo-Volcanological Setting

Volcanism has been occurring in the Campi Flegrei volcanic area, which encircles the western portion of Naples Bay, since 50 ky B.P. With a diameter of 12 km^2 (a Phlegrean caldera), Campi Flegrei is a resurgent caldera [50–61] that was created by the volcanic–tectonic collapse brought on by the volcanic eruption of the pyroclastic flow deposits of the Campanian Ignimbrite (37 ky B.P.) [62–73]. Following the eruption of the Campanian Ignimbrite pyroclastic flow deposits, the volcanic–tectonic collapse of the caldera itself controlled the individuation of the submerged margin of the Phlegrean caldera, which is represented by the Gulf of Pozzuoli. Coastal deposits, ranging in age from 10 ky B.P. to 5.3 ky B.P., crop out at about 50 m above sea level at La Starza marine terrace (Gulf of Pozzuoli), indicating a volcanic–tectonic uplift of the caldera center [44,45,59].

The monogenetic volcanic edifices are coincident with the submerged caldera rim representing relict volcanic morphologies, characterized by polycyclic erosional surfaces, cropping out at the seafloor, carving the volcanic deposits and overlain by Holocene sediments, which are highly variable in thickness (Figure 4). In these sections, volcanic edifices are mixed with sedimentary units (Figure 4), as in the case of the Procida Channel (inset a) and the Gulf of Pozzuoli (inset b and c).

The geology and stratigraphy of the Phlegrean Fields were summarized by Rosi and Sbrana [50] and then updated by Sbrana et al. [74]. The graben of the Campania Plain is in a central position in Campi Flegrei, which is a Quaternary volcanic area. A huge caldera, known as the Phlegrean caldera (Figure 5), which was designated after the volcanic–tectonic collapse that occurred after the eruption of the Campanian Ignimbrite, serves as the primary structural element. Up until historical times, there was continuous volcanic activity inside the Phlegrean caldera and around its edges. Small, dispersed volcanic structures that release pyroclastic deposits and lavas are the sites of pre-caldera volcanic activity.

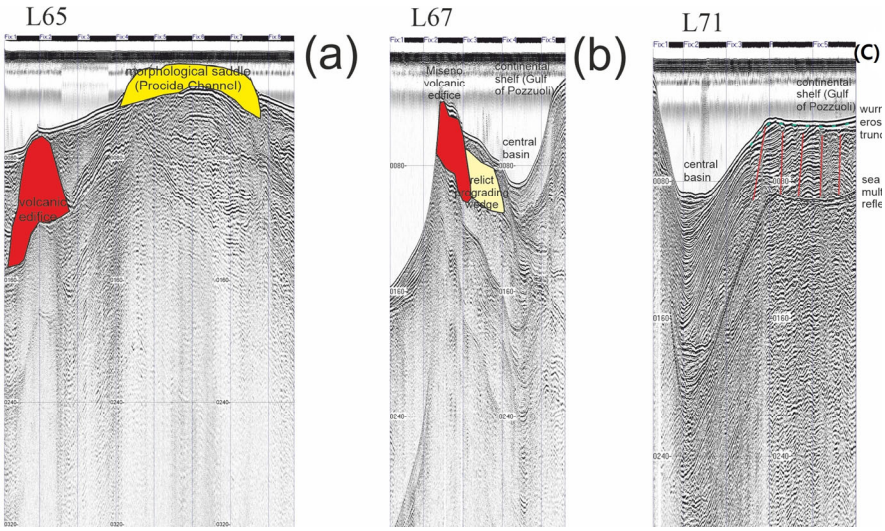

Figure 4. Composite sketch diagram of the seismic sections of the Ischia offshore and the Gulf of Pozzuoli, showing significant seismic sections collected in the two areas (inset (**a**): Ischia offshore; inset (**b**,**c**): Gulf of Pozzuoli. Shot points are reported on the horizontal scale, while two-way times are reported on the vertical scale. Red lines in the inset (**c**) represent small-scale normal faults.

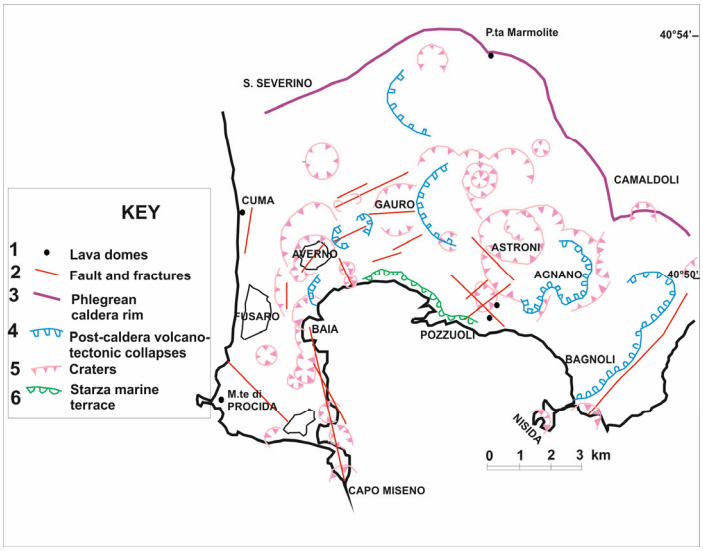

Figure 5. Geologic and geomorphologic sketch map of the Gulf of Pozzuoli (modified from Aiello et al.) [27]. Black line indicates the coastline.

The corresponding outcrop, located at the coastal cliff of M.te di Procida (Figure 6; https://www.facebook.com/photo/?fbid=1015372813977389&set=pcb.1015372903977380; accessed on 1 August 2025), shows a thick pyroclastic sequence with interlayered paleosols. The post-caldera activity has developed in four main phases, identified through radiometric determinations and paleogeographic evolution, from 37 ky B.P. to historical times.

The oldest phase was established based on the stratigraphy of deep wells in the Phlegrean area (geothermal areas of Mofete and San Vito; Figure 7) and includes thick volcaniclastic deposits (tuffs) interlayered with minor lava bodies, covered by large yellow tuff outcrops. The second, third, and fourth eruptive phases between 10.5 ky and 1538 A.D. produced subaerial deposits separated by paleosols [56].

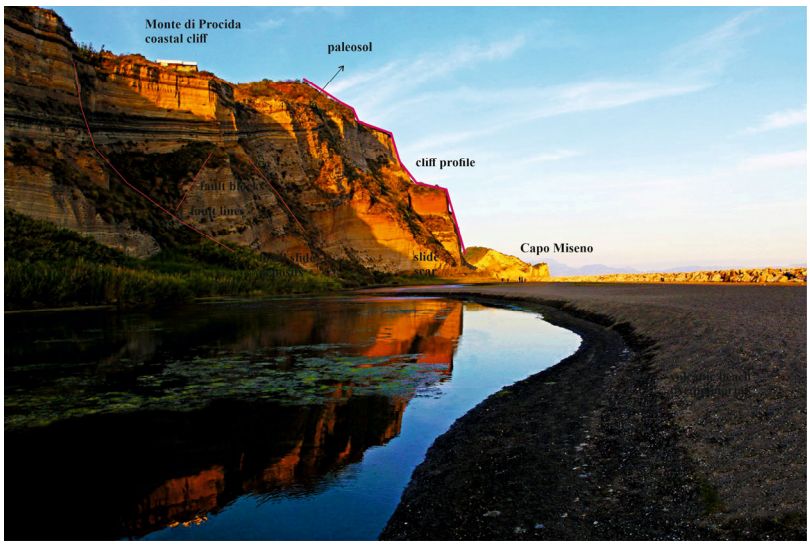

Figure 6. The coastal cliff of Monte di Procida (Gulf of Naples, Italy https://www.facebook.com/photo/?fbid=1015372813977389&set=pcb.1015372903977380, accessed on 1 August 2025). Note the occurrence of several paleosols interstratified in the volcanic sequence.

The stratigraphy of the Campi Flegrei volcanic complex has been further refined by Sbrana et al. (Figure 8) [74]. A new volcanological map of the Campi Flegrei volcanic complex, coupled with the Procida Island, has been synthesized, showing the geological and volcanological evolution of the region. This map, at the 1:25,000 scale, represents the volcanic and structural evolution of the area, showing both the phases of activity and the phases of quiescence, and is based on up-to-date geological and seismo-stratigraphic data, with a focus on the evolutionary history of the volcanic field. As a result of the construction of this map, seven phases of volcanic activity have been recognized, representing the evolution history of the area, which have been integrated with the Roman archeological data, to analyze the processes of subsidence and uplift in the area [74]. Based on volcanological data, the Campi Flegrei caldera was formed around 39.3 ky B.P., after the eruption of the Campanian Ignimbrite, which has significantly impacted the volcanic structure. Moreover, the map shows the fault systems that influenced the collapse and the successive evolution of the caldera. Moreover, a renewal of the caldera evolution has been suggested at about 12 ky B.P. Seven phases of volcanic activity have been identified based on the up-to-date data on the volcanic eruptions, showing periods of volcanism alternating with phases of quiescence. Each phase is characterized by distinctive characteristics and different impacts on the morphology of the area. The first phase corresponds to the ancient volcanic field with monogenetic volcanoes, including the Ischia regional markers, the Epomeo welded ignimbrites, and the Pignatiello Plinian tephra layers (Figure 8) [74]. The second phase corresponds to the eruption of the Campanian Ignimbrite and the caldera formation, which are genetically related. The third phase corresponds to the intra-caldera volcanic activity, with submarine eruptions, including the Posillipo and Gauro multivent hydromagmatic eruptions, and the post-NYT (Neapolitan Yellow Tuffs) caldera collapses, including Bagnoli, San Vito, and Toiano. On the Procida Island, the Solchiaro tuff ring was formed, before the NYT eruption, due to the contemporaneous activity of the Gauro and Posillipo tuff cones. The fourth phase corresponds to the activity of tuff rings, tuff cones, and Plinian and sub-Plinian eruptions. The activity of tuff rings and tuff cones continued during the fifth phase. The sixth phase corresponds to recent volcanic activity, with the formation of the Capo Miseno tuff cone and the Plinian eruption, namely Agnano-Monte Spina [74]. Finally, the seventh phase is distinguished from the eruption of M.te Nuovo in 1538 A.D.

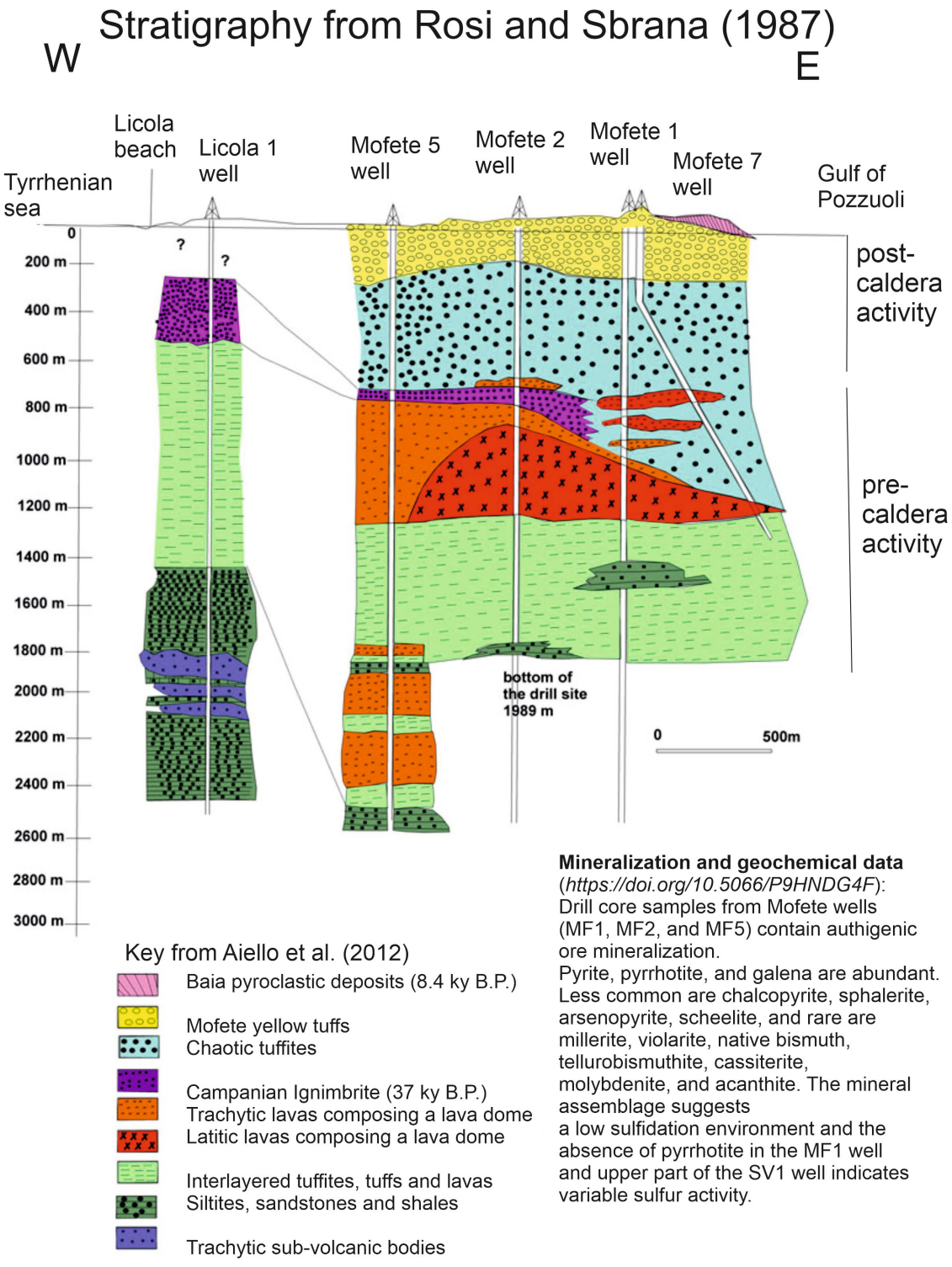

Figure 7. Stratigraphy and geochemistry of the geothermal area of Mofete (Phlegrean Fields). The stratigraphic data are modified from Rosi and Sbrana (1987) [50] and Aiello et al. (2012) [26]. The mineralization and geochemical data have been modified from https://doi.org/10.5066/P9HNDG4F (accessed on 19 May 2025) and have been provided by Harvey Belkin, Ryan McAleer, Benedetto De Vivo, and Mary R. Croke (record source: https://www.usgs.gov/ais; accessed on 1 August 2025).

Table 2. Volcanic phases and corresponding details of Campi Flegrei volcanologic evolution (modified from Sbrana et al.) [74].

Phase 1: Pre-caldera activity	Oldest trachytic volcanoes of Miliscola and Vita Fumo. Spatters and lava domes of S. Martino. Torregaveta lava field (Monte di Procida). Pignatiello Formation. Ischia regional markers. Lava dome of Cuma. San Severino quarries (PDCs). Punta Marmolite deposits. Northern border of Quarto plain. Volcanic deposits of the Camaldoli hill. Torre di Franco tuffs. White tuffs. Volcanic deposits of the Naples town: San Martino hill, Funicolare di Chiaia, Parco Grifeo, Parco Margherita, San Sepolcro, M.te Echia, Castel dell'Ovo, Capodimonte, Soccavo, Camaldoli. Volcanic tuff rings and tuff cones at Fiumicello and Vivara.
Phase 2: Campanian Ignimbrite eruption and genetically related caldera formation	Campanian Ignimbrite proximal deposits, including a trachytic to phonolitic Plinian fallout layer, followed by densely welded and welded trachytic ignimbrites. Piperno. Campanian Grey Tuffs. Breccia Museo (lithic breccias) is composed of ash and pumice-rich PDC deposits, which were erupted during the phase of caldera collapse.
Phase 3: Neapolitan Yellow Tuff eruption (NYT)	Posillipo and Gauro multivent hydromagmatic eruptions. Post-NYT nested collapses. CI caldera fills with marine deposits during the first stages. Trentaremi, Torregaveta and Monticelli volcanic vents.
Phase 4: Resurgence of the caldera center and volcanism in correspondence with numerous volcanic edifices	Deposition of coastal and marine sands on the La Starza marine terrace (Gulf of Pozzuoli). Emplacement of minor tuff cones, including the Nisida Bank, Bacoli tuff cone, S. Teresa tuff cone, Porto Miseno tuff cone, Minopoli scoria vent, Pisani ash ring, La Pietra tuff cone, Montagna Spaccata scoria and spatter cone, Fondo Riccio scoria and spatter cone, Concola scoria and spatter cone. Pomici Principali Plinian eruption (PDCs).
Phase 5: Eruption in correspondence with a few volcanic edifices	Deposition of coastal and marine sands on the La Starza marine terrace (Gulf of Pozzuoli). Eruption of the Baia and Fondi di Baia tuff rings (including the Procida Island). Lava flow of Monte Spina. Spattered eruptions in the caldera center, including the Costa S. Domenico and S. Martino tuff rings.
Phase 6: Collapse of the nested caldera, deposition of marine sediments, Plinian eruptions and volcanic eruptions	Deposition of the post-AMS shore sediments. The volcanic eruption corresponded with the Capo Miseno tuff cone. Plinian eruption of Agnano-Monte Spina. Emplacement of the Olibano and Accademia volcanic domes. Volcanic activity of the Solfatara maar. Astroni, Senga and Nisida volcanoes.
Phase 7: Renewal of volcanic activity and caldera uplift	Eruption of the Monte Nuovo volcanic edifice. Volcanic–tectonic uplift of the caldera center in correspondence with a volcanic dome.

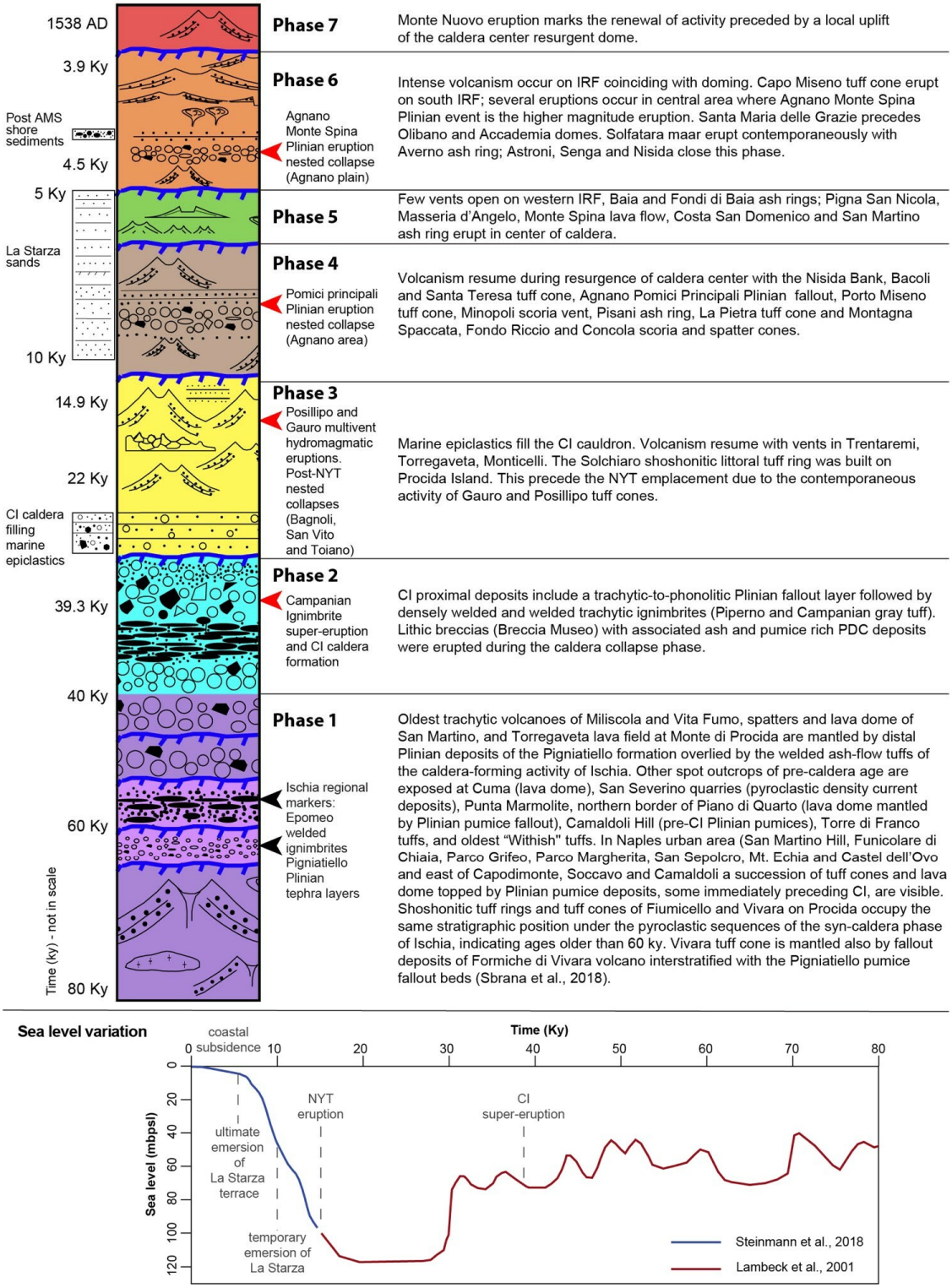

Figure 8. Stratigraphy of the Phlegrean Fields volcanic complex (modified from Sbrana et al.) [74]. For the details of the volcanic phases, refer to Table 2.

The details of the volcanic eruptions occurring in the seven phases are reported in Table 2.

The sea level fluctuations have significantly impacted the volcanological evolution and morphology of the Phlegrean Fields (Figure 8) [74]. The archeological features show that Roman structures have been influenced by these changes. During the last 2 ky, the observed sea level fluctuations include a sea level rise of more than 2 m at Pozzuoli, and a

sea level fall between 6 and 8 m at Baia. Moreover, submerged abrasion terraces have been observed at several water depths. The CI caldera has been influenced by two important ring faults, namely the Outer Ring Fault (ORF) and the Inner Ring Fault (IRF) [60,61,74]. In correspondence with these ring faults, clusters of volcanoes have been active. In particular, the third phase mentioned in Table 2 [74] corresponded with a significant volcanic activity along the ring fault, namely ORF, while the volcanic activity was scattered in phase 4 (Table 2). The fourth, fifth, and sixth phases are mainly related to the Inner Ring Fault, namely the IRF. The caldera resurgence started during the fourth phase, with structures of resurgent domes, occurring both onshore and offshore [60,61,75]. Natale et al. [75] have highlighted that the eruption of the NYT deposits was followed by intense intra-caldera activity, and by the resurgence of a central dome. The structural framework of this dome has been divided into two main parts, including a northern group of normal faults, with an E-W to WNW-ESE strike, occurring on the continental shelf of Pozzuoli, and forming a horst and graben structure. Moreover, the trend and the extension of the first set of faults are in overall agreement with the youngest fractures, which have been mapped onshore in the emerged part of the resurgent dome [76–78].

4. Seismo-Stratigraphic Framework

The seismo-stratigraphic framework has been reconstructed through the geological interpretation of a grid of high-resolution seismic profiles recorded in the frame of the geological and technical activities for the realization of the geological sheet n. 446–447 Napoli, at the 1:50.000 scale (https://www.isprambiente.gov.it/Media/carg/447_NAPOLI/Foglio.html; accessed on 1 August 2025). The seismic sections available for geological interpretation (Figure 1) [26] consist of three dip lines (perpendicular to the shoreline), L67_07, L73_07, and L74_07, and five tie lines (parallel to the shoreline), L68_07, L69_07, L70_07, L71_07, and L72_07.

The seismic sections for the geological interpretation have been selected taking into account the areas where gas or fluids possibly occur. These sections are L67_07, L68_07, L72_07, and L74_07. Seismic signatures of gas and gas criteria, including the enhanced reflections, are briefly analyzed. Acoustic turbidity, amplified (enhanced) reflections, columnar disturbances or gas chimneys, and acoustic blanking are the primary forms of seismic evidence [2]. A pull-down of seismic reflections in the presence of gas is frequently linked to acoustic turbidity, which is defined by chaotic reflections that are regulated by the dispersion of acoustic energy. For a portion of their extent, the amplified (enhanced) reflections are reflected by coherent seismic reflections with an increased amplitude, which can indicate the lateral extension of acoustic turbidity zones. While porous silty and sandy deposits are linked to heightened reflections, fine-grained sediments that are rich in clays are characterized by acoustic turbidity. The limitations of the Sparker profiles in the seismic interpretation of gas features are their resolution and the fact that bright spots are often detected. Low-resolution Sparker data may prevent their identification.

The L67_07 seismic profile, whose geological interpretation is reported in Figure 9, shows the seismo-stratigraphic setting of the Gulf of Pozzuoli in correspondence to the Miseno Cape tuff cone.

The corresponding volcanic edifice is shown in the lower part of the figure (Figure 9). The Capo Miseno tuff cone pertains to the post-CI caldera tuff cones, deposited during the sixth phase [74]. The sixth phase is distinguished from recent intra-caldera Holocene activity due to the opening of 12 volcanic vents [79].

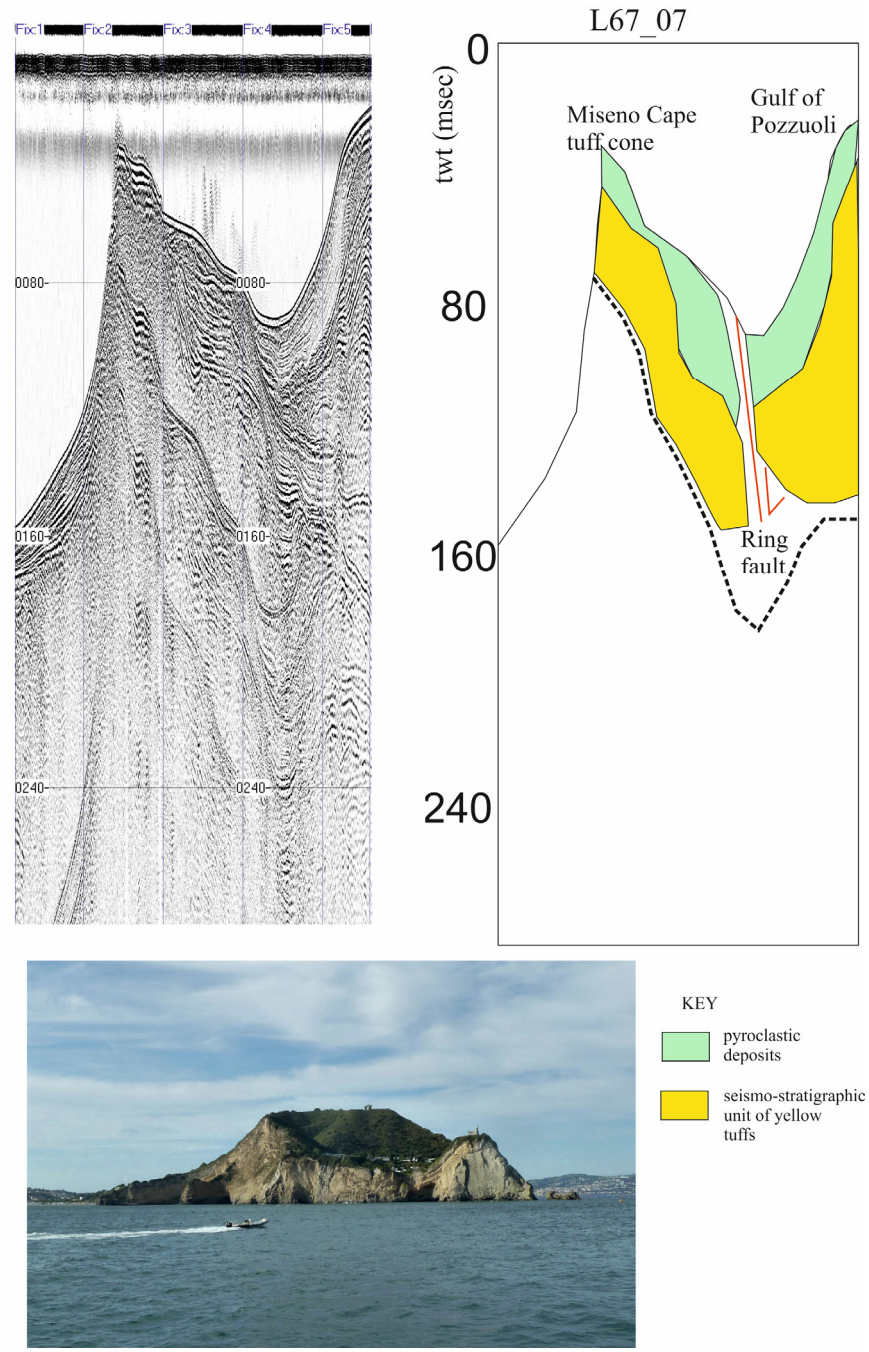

Figure 9. Sparker profile L67_07 and corresponding geological interpretation. In the first picture, shot points are reported on the horizontal scale, and two-way travel times are reported on the vertical scale.

Two main seismo-stratigraphic units occur: the pyroclastic deposits and the seismo-stratigraphic unit of yellow tuffs (Figure 9). Moreover, an important fault has been identified on the seismic profile, probably corresponding to the Inner Ring Fault, bounding the inner margins of the caldera structure (Figure 9) [60,61,78].

The geological interpretation of the seismic profile L68 shows the fluid uprising in correspondence with anticlines, deforming the marine deposits (Figure 10). The fluid uprising is suggested by the occurrence of acoustically transparent vertical zones, interrupting the lateral continuity of the marine record (Figure 10). Both marine and volcanic seismo-stratigraphic units have been identified (Figure 10). The lowermost unit, interpreted as a pyroclastic unit, whose attribution is uncertain, is deformed by anticlinalic structures, namely three anticlines which are separated by two synclines (Figure 10). These structures

could be genetically related to the resurgent dome occurring in the area, as highlighted by previous studies [18,59–61,75–78]. Other important seismo-stratigraphic units include the Neapolitan Yellow Tuff (NYT), occurring from the Nisida inlet to the Nisida slope (Figure 10), and the tuff cones of the Nisida complex (Figure 10).

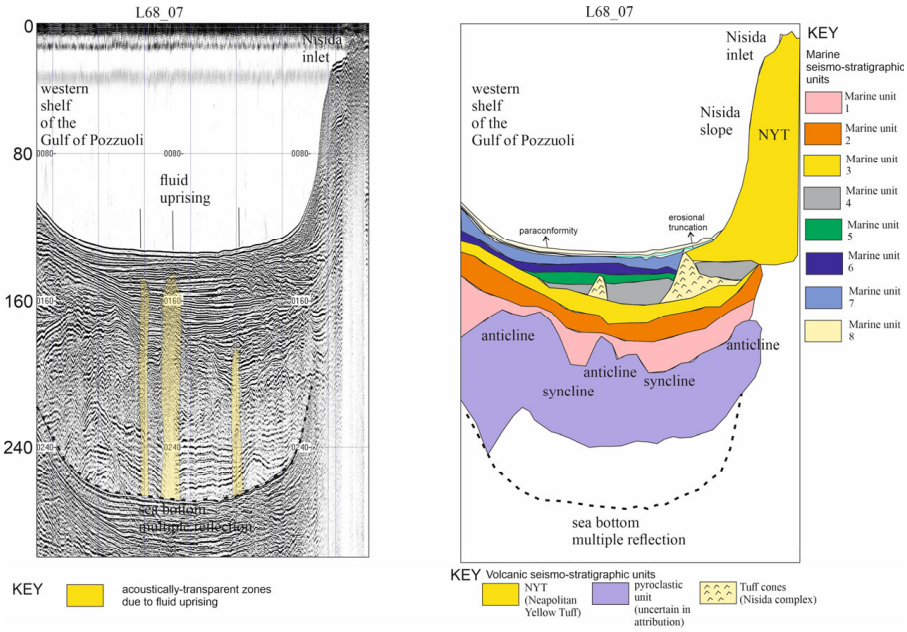

Figure 10. Sparker profile L68_07 and corresponding geological interpretation. In the first picture, shot points have been reported on the horizontal scale, while two-way travel times have been reported on the vertical scale.

A detailed geological interpretation of the Pleistocene–Holocene marine record has been carried out, allowing for the identification of eight seismo-stratigraphic units (Figure 10). The lowermost one (1 in Figure 10) infills the deep depressions identified at the top of the underlying pyroclastic unit. Two other units (2 and 3 in Figure 10), characterized by oblique to parallel reflectors, overlie the first seismo-stratigraphic unit of the marine record (Figure 10). The fourth seismo-stratigraphic unit has a wedge-shaped external geometry, and is interlayered with the mounded unit of the Nisida volcanic complex (Figure 10). Units 5, 6, and 7 complete the basin filling of the Gulf of Pozzuoli. Their upper part is truncated by an erosional unconformity, towards Nisida (Naples), grading into a paraconformity towards Pozzuoli (Figure 10).

A similar stratigraphic architecture has been detected in the seismic profile L69_07 (Figure 11). Two zones of fluid uprising have been detected in correspondence with two synclinal structures, highlighting that the fluids may have been concentrated in the depressed areas (Figure 11).

The seismic profile L72_07 shows an acoustically transparent body associated with fluid uprising, an anticlinalic structure, and progradational bodies genetically related to the last glacio-eustatic sea level cycle (Figure 12).

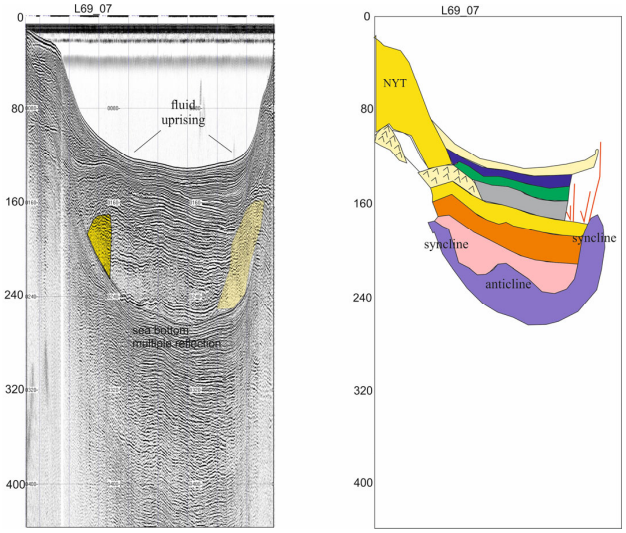

Figure 11. Sparker profile L69_07 and corresponding geological interpretation. For the key, see Figure 10. In the first picture, shot points have been reported on the horizontal scale, while two-way travel times have been reported on the vertical scale.

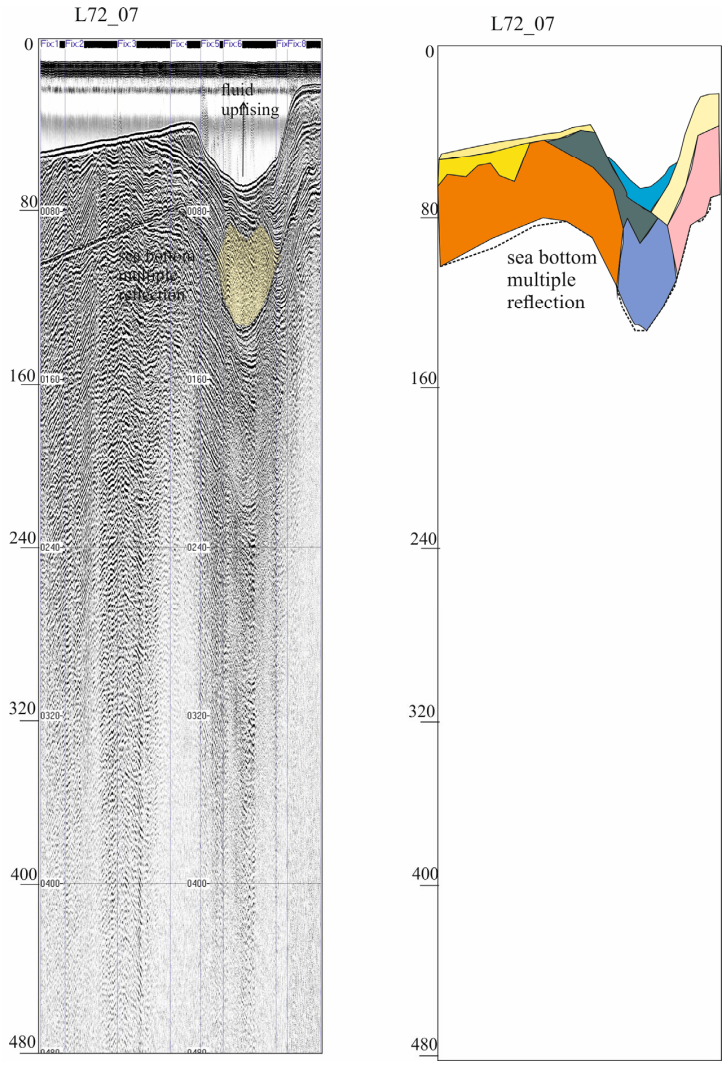

Figure 12. Sparker profile L72_07 and corresponding geological interpretation. For the key, see Figure 10. In the first picture, shot points have been reported on the horizontal scale, while two-way travel times have been reported on the vertical scale.

5. Discussion

Fluid uprising in correspondence with anticlinalic and synclinalic structures has been highlighted based on geological interpretation of seismic profiles. Different geological interpretations have been shown for these seismic sections by Aiello et al. [26] and by Sbrana et al. [74]. For the comprehension of the stratigraphic setting of the area, it is useful to keep in mind the reported geological interpretations, which are respectively compiled in Table 3 [26] and in Table 4 [74].

Table 3. Seismo-stratigraphic framework of the Gulf of Pozzuoli based on Aiello et al. [26].

Seismo-Stratigraphic Unit	Seismic Facies	Geological Interpretation	Location
HST	Progradational to parallel seismic reflectors	Highstand system tract	Eastern sector of the Gulf of Pozzuoli
TST	Retrogradational seismic reflectors	Transgressive system tract	Eastern sector of the Gulf of Pozzuoli
Lsl	Wedge-shaped, chaotic to discontinuous seismic unit	Landslide deposits intercalated in the upper part of the Lowstand System Tract; local occurrence of paleo-channels	Gulf of Pozzuoli (southwards of the Miseno Cape)
LST	Progradational seismic reflectors, erosionally truncated at their top	Lowstand System Tract	Inner continental shelf (Gulf of Pozzuoli)
G1	Parallel and continuous seismic reflectors	Upper sedimentary unit of the basin fill, attaining maximum thickness in the depocenter of the central basin	Gulf of Pozzuoli
lsl2	Wedge-shaped, chaotic to discontinuous seismic unit	Fossil landslide overlying the G2 marine unit and underlying the LST deposits	Eastern sector of the Gulf of Pozzuoli
NYT/PC	NYT: wedge-shaped acoustically transparent volcanic seismic unit	NYT: pyroclastic deposits of the Neapolitan Yellow Tuff (15 ky B.P.) PC: Tuff cones of the Nisida volcanic complex in facies with the Neapolitan Yellow Tuffs and interstratified with the G3 marine deposits.	Gulf of Naples Gulf of Pozzuoli
G2	Parallel and continuous seismic reflectors	Intermediate seismic unit of the basin fill; deformed in correspondence with growth anticlines (Punta Pennata anticline, Pozzuoli anticline, Nisida anticline) and synclines (central syncline of the Gulf of Pozzuoli, Epitaffio syncline).	Gulf of Pozzuoli
Lsl1	Wedge-shaped, chaotic to discontinuous seismic unit	Wide paleo-landslide, overlying the V3 volcaniclastic unit and coeval with the basal part of the G2 marine unit	Eastern sector of the Gulf of Pozzuoli

Table 3. *Cont.*

Seismo-Stratigraphic Unit	Seismic Facies	Geological Interpretation	Location
Pyr 2	Continuous progradational to parallel seismic reflectors	Pyroclastic unit deposited from Capo Miseno to the Miseno Bank; deformed by wedging and growth in correspondence with normal faults.	Eastern sector of the Gulf of Pozzuoli
Dk	Sub-vertical volcanic bodies, acoustically transparent, locally bounded by normal faults	Volcanic dykes controlled by the magma uprising in correspondence with normal faults	Eastern and central sectors of the Gulf of Pozzuoli
Pyr1	Discontinuous to sub-parallel seismic reflectors	Pyroclastic unit filling a structural depression under the Miseno Cape volcanic edifice	Eastern sector of the Gulf of Pozzuoli
G3	Discontinuous to parallel seismic reflectors	Lower seismo-stratigraphic unit; deformed in correspondence to anticlines and synclines	Gulf of Pozzuoli
V3	Acoustically transparent to discontinuous seismic unit; strongly eroded at its top	Volcaniclastic unit deposited at the northern margin of the Pentapalummo Bank	Gulf of Pozzuoli

Table 4. Seismo-stratigraphic framework of the Gulf of Pozzuoli based on Sbrana et al. [74].

Seismo-Stratigraphic Units and Other Significant Features	Seismic Facies	Geological Interpretation	Location
Lower seismo-stratigraphic unit	Spaced plane parallel reflections	Marine epiclastic (fossil reworked tuffs) drilled at the Mofete and San Vito geothermal areas under yellow tuffs of Phase 3 (post Campanian Ignimbrite?)	Seismic sections L68, L69, L71, L74
Seismo-stratigraphic unit, overlying the lower one	Irregular surface at its top, with hummocks and V-shaped surfaces, variable lateral thickness, discontinuous internal reflectors.	Landslide deposits older than the NYT deposits	Seismic sections L68, L69; L71; L74
Seismo-stratigraphic unit of phase 3 of Sbrana et al. [74]	Well-stratified seismic unit	NYT (Neapolitan Yellow Tuff), Posillipo vent alignment, Gauro hydromagmatic tuff cone deposits. Involved in the dome-shaped resurgence of the central collapsed portion of the caldera.	All the seismic sections of the available grid
Outer and Inner Ring Faults allowing for the caldera collapse.			
Three orders of marine abrasion surfaces (90–110 m, 60 m, 40 m, 20–30 m)			

Aiello et al. [26] have shown fourteen seismic units in the Gulf of Pozzuoli (Table 4), while different units have been highlighted by Sbrana et al. [74], according to the seven phases of geological evolution of the volcanic complex (Table 3). Geological interpretation has identified 14 seismic units, including volcanic and sedimentary, that are tectonically governed by normal faulting and concurrent folding.

Locally restricted by normal faults, volcanic dykes are characterized by acoustically transparent sub-vertical masses that indicate magma rising in accordance with extensional processes [26] (Table 3). The emplacement of the Neapolitan Yellow Tuff deposits (Nisida volcanic complex) is associated with a field of tuff cones interlayered with marine deposits off Nisida island, on the western border of the Gulf. The Bacoli-Isola Pennata-Capo Miseno yellow tuffs that appear in the northern Phlegrean Fields are connected to a thick tabular volcanic unit off the Capo Miseno volcanic edifice that was previously unknown [26] (Table 3). Seismic profiles have identified large underwater slides that are associated with important submerged instability mechanisms. Theoretically, pyroclastic flow and surges associated with the 3.8 ka old Averno eruptions that entered the sea and the Monte Nuovo eruptions in 1538 A.D. should cause these landslides [26] (Table 3).

Sbrana et al. [74] have related the seismo-stratigraphic units to a volcanological phase (phase 3) [74] (Table 4). The third phase includes important volcanic edifices and volcanic seismo-stratigraphic units, such as the Neapolitan Yellow Tuff (NYT), the Posillipo vent alignment, and the Gauro hydromagmatic tuff cone deposits [74]. The underlying seismo-stratigraphic units are genetically related to the first phases of caldera filling [74] (Table 4). During phase 2, the Campanian Ignimbrite (CI) deposits erupted and the CI caldera was formed [74], but the depth of the available seismic sections has not allowed the identification of the CI seismo-stratigraphic unit, which is well constrained [26,27,55,59–61].

Resurgent dome faults have been recognized based on the interpretation of seismic sections offshore of Campi Flegrei [75]. In this region, Natale et al. [75] focused on the occurrence of volcanic–tectonic faults based on seismo-stratigraphic interpretation. The gravity cores, previously published [59], have been used to calibrate the upper stratigraphic interval. Important stratigraphic markers occur in this interval, including (from the youngest to the oldest) the 1538 C.E. Monte Nuovo tephra, the 79 C.E. tephra (genetically related to the Somma-Vesuvius) mixed with the 60 C.E. Cretaio eruption (Ischia Island), and finally, a tephra dated at ~3.9 kyr correlated to Nisida or Capo Miseno. Tephra interlayered with marine deposits has been correlated with seismic reflectors characterized by high amplitude and high frequency. In this sequence, alternating sandy and silty deposits and ash/pumice/lithic layers control strong variations of acoustic impedance in the stratigraphic sequence. Volcaniclastic deposits, alternating with marine deposits, have also been recognized and interpreted based on acoustically transparent or chaotic seismic reflectors.

In the Gulf of Pozzuoli, the chronostratigraphic framework of the caldera infill sequence has been reconstructed and calibrated by the NYT depth [60,61]. In particular, the seismic reflectors with a high amplitude have been interpreted as tephra deposits, corresponding with significant volcanic events, while the acoustically transparent intervals have been interpreted as marine deposits, with a subordinate volcaniclastic fraction [75].

6. Conclusions

The main conclusions are as follows:

- Fluid uprising is shown by acoustically transparent zones, previously interpreted as volcanic sequences.
- Fluid uprising is concentrated in anticlinalic and synclinalic structures. This finding is in agreement with previous studies on reservoir characterization, showing that these

structures represent structural and stratigraphic traps [80]. In particular, roll-over anticlines represent valuable stratigraphic traps in hydrocarbon exploration.

- Seismo-stratigraphic data suggest that the fluid uprising could be genetically related to the new bradyseismic crisis in the Gulf of Pozzuoli, still in course, as suggested by earthquakes and bradyseism occurring in this area, both onshore and offshore.
- This phenomenon can be compared with similar processes on the fluid uprising controlling the individuation of seabed domes in the Naples Bay, namely the Banco della Montagna feature [11]. Active degassing has also been singled out.
- In this volcanic–tectonic framework, the suggested mechanism is controlled by the occurrence of a heat source (magma reservoir) in the continental crust and/or the mantle, genetically related to the occurrence of submerged hydrothermal discharges in the Campania coastal regions.
- Identifying (a) morphologies associated with active seabed deformation and (b) gas emissions close to heavily populated coastal regions, such as Italy's Neapolitan volcanic area (home to approximately 1 million people), is crucial for assessing the likelihood of shallow-depth volcanic eruptions.

The main limitation is the lack of a systematic network of geochemical and sedimentological data constraining the suggested mechanism. Geochemical data have been collected onshore in the Solfatara–Pisciarelli geothermal system, but systematic data collection is still lacking offshore. Prior to and during the 1982–1984 bradyseismic crisis and the three minor events, there were significant differences in the concentrations of fumarolic effluents' major and minor gas species. Specifically, the H_2O/CO_2 and S/C ratios gradually increased before each deformation episode, and they sharply decreased afterward [4]. These consistent alterations implied that the processes controlling ground deformation and hydrothermal circulation must be related in some way. Measurements of diffuse degassing, which for the first time demonstrated the remarkable scale of this process, validated the importance of fluid and heat transmission at La Solfatara [4,15].

At the same time, marine gravity cores, previously published in the Gulf of Pozzuoli, are scattered [59], and consequently, the sedimentological data must be improved. These data are limited to the gravity cores C1062, C32, and C23 [59]. The facies analysis has shown bioturbated muds, with interlayered coarse-grained layers, mostly consisting of sandy silt rich in bioclasts and/or volcaniclasts, along with three important tephra layers [59]. A denser network of marine gravity cores in the Gulf of Pozzuoli needs to be acquired in future geological and geophysical studies using the R/V Gaia Blu of the National Research Council of Italy.

Future work and suggestions include the acquisition of a dense network of geochemical and sedimentological data to solve the geological problem of the relationships between gas and bradyseism in the Gulf of Pozzuoli, and possibly, the acquisition of a densely spaced grid of seismic profiles (Sparker or multichannel) to improve the seismic interpretation of the gas features.

Funding: This research received no external funding.

Data Availability Statement: No new data were created or analyzed in this study.

Conflicts of Interest: The author declares no conflicts of interest.

References

1. Carlson, P.R.; Golan-Bac, M.; Karl, H.A.; Kvenvolden, K.A. Seismic and geochemical evidence for shallow gas in sediment of Navarin continental margin, Bering Sea. *AAPG Bull.* **1985**, *69*, 422–436. [CrossRef]
2. Judd, A.G.; Hovland, M. The evidence of shallow gas in marine sediments. *Cont. Shelf Res.* **1992**, *12*, 1081–1095. [CrossRef]

3. Lee, S.H.; Chough, S.K. Distribution and origin of shallow gas in deep-sea sediments of the Ulleung Basin, East Sea (Sea of Japan). *Geo-Mar. Lett.* **2003**, *22*, 204–209. [CrossRef]
4. Todesco, M.; Chiodini, G.; Macedonio, G. Monitoring and modelling hydrothermal fluid emission at La Solfatara (Phlegrean Fields, Italy). An interdisciplinary approach to the study of diffuse degassing. *J. Volcanol. Geoth. Res.* **2003**, *125*, 57–79. [CrossRef]
5. Chiodini, G.; Avino, R.; Brombach, T.; Caliro, S.; Cardellini, C.; De Vita, S.; Frondini, F.; Granirei, D.; Marotta, E.; Ventura, G. Fumarolic and diffuse soil degassing west of Mount Epomeo, Ischia, Italy. *J. Volcanol. Geoth. Res.* **2004**, *133*, 291–309. [CrossRef]
6. Castellarin, A.; Rabbi, E.; Cremonini, S.; Martelli, L.; Piattoni, F. New insights into the underground hydrology of the eastern Po Plain (northern Italy). *Boll. Geof. Teor. Appl.* **2006**, *47*, 271–298.
7. Bruno, P.P.G.; Ricciardi, G.P.; Petrillo, Z.; Di Fiore, V.; Troiano, A.; Chiodini, G. Geophysical and hydrogeological experiments from a shallow hydrothermal system at Solfatara Volcano, Campi Flegrei, Italy: Response to caldera unrest. *J. Geophys. Res.* **2007**, *112*, B06201. [CrossRef]
8. Hovland, M. The Geomorphology and Nature of Seabed Seepage Processes. In *Bathymetry and Its Applications*; Blondel, P., Ed.; IntechOpen: Rjeka, Croatia, 2012; Chapter 4; pp. 79–104.
9. Italiano, F.; Liotta, M.; Martelli, M.; Martinelli, G.; Petrini, R.; Riggio, A.; Rizzo, A.L.; Slejko, F.; Stenni, B. Geochemical features and effects on deep-seated fluids during the May-June 2012 southern Po Valley seismic sequence. *Ann. Geophys.* **2012**, *55*, 815–821. [CrossRef]
10. Piochi, M.; Kilburn, C.R.J.; Di Vito, M.A.; Mormone, A.; Tramelli, A.; Troise, C.; De Natale, G. The volcanic and geothermally active Campi Flegrei caldera:an integrated multidisciplinary image of its buried structure. *Int. J. Earth Sci.* **2014**, *103*, 401–421. [CrossRef]
11. Passaro, S.; Tamburrino, S.; Vallefuoco, M.; Tassi, F.; Vaselli, O.; Giannini, L.; Chiodini, G.; Caliro, S.; Sacchi, M.; Rizzo, A.L.; et al. Seafloor doming driven by degassing processes unveils sprouting volcanism in coastal areas. *Sci. Rep.* **2016**, *6*, 22448. [CrossRef]
12. Aiello, G.; Insinga, D.D.; Iorio, M.; Meo, A.; Senatore, M.R. On the occurrence of the Neapolitan Yellow Tuff tephra in the Northern Phlegraean Fields offshore (Eastern Tyrrhenian margin; Italy). *Ital. J. Geosci.* **2017**, *136*, 263–274. [CrossRef]
13. Siniscalchi, A.; Tripaldi, S.; Romano, G.; Chiodini, G.; Improta, L.; Petrillo, Z.; D'Auria, L.; Caliro, S.; Avino, R. Reservoir structure and hydraulic properties of the Campi Flegrei geothermal system inferred by audiomagnetotelluric, geochemical, and seismicity study. *J. Geophys. Res. Solid Earth* **2019**, *124*, 5336–5356. [CrossRef]
14. Ismail, A.; Ewida, H.F.; Al-Ibiary, M.G.; Gammaldi, S.; Zollo, A. Identification of gas zones and chimneys using seismic attributes analysis at the Scarab field, offshore, Nile Delta, Egypt. *Pet. Res.* **2020**, *5*, 59–69. [CrossRef]
15. Isaia, R.; Di Giuseppe, M.G.; Natale, J.; Tramparulo, F.D.A.; Troiano, A.; Vitale, S. Volcano-tectonic setting of the Pisciarelli fumarole field, Campi Flegrei caldera, southern Italy: Insights into fluid circulation patterns and hazard scenarios. *Tectonics* **2021**, *40*, e2020TC006227. [CrossRef]
16. Aiello, G.; Caccavale, M. New Seismoacoustic Data on Shallow Gas in Holocene Marine Shelf Sediments Offshore from the Cilento Promontory (Southern Tyrrhenian Sea, Italy). *J. Mar. Sci. Eng.* **2022**, *10*, 1992. [CrossRef]
17. Torrese, P. ERT investigation of mud volcanoes: Detection of mud fluid migration pathways from 2D and 3D synthetic modeling. *Acta Geod. et Geophys.* **2023**, *58*, 601–629. [CrossRef]
18. Vitale, S.; Natale, J. Combined volcano-tectonic processes for the drowning of the Roman western coastal settlements at Campi Flegrei (southern Italy). *Earth Planets Space* **2023**, *75*, 38. [CrossRef]
19. Carfagna, N.; Brindisi, A.; Paolucci, E.; Albarello, D. Seismic monitoring of gas emissions at mud volcanoes: The case of Nirano (northern Italy). *J. Volcanol. Geoth. Res.* **2024**, *446*, 107993. [CrossRef]
20. Brindisi, A.; Paolucci, E.; Carfagna, N.; Albarello, D. Passive seismic measurements to characterize gas reservoirs in a mud volcano field in Northern Italy. *Mar. Petrol. Geol.* **2025**, *173*, 107275. [CrossRef]
21. Spatola, D.; Dahal, A.; Lombardo, L.; Casalbore, D.; Chiocci, F.L. First Pockmark susceptibility map of the Italian continental margins. *Mar. Petrol. Geol.* **2025**, *176*, 107337. [CrossRef]
22. Gammaldi, S.; Ismail, A.; Zollo, A. Fluid Accumulation Zone by Seismic Attributes and Amplitude Versus Offset Analysis at Solfatara Volcano, Campi Flegrei, Italy. *Front. Earth Sci.* **2022**, *10*, 866534. [CrossRef]
23. Iorio, M.; Meo, A.; Aiello, G.; Senatore, M.R. The Neapolitan Yellow Tuff record in the Gaeta Gulf (Eastern Tyrrhenian margin, Southern Italy). *Adv. Geosci.* **2024**, *63*, 15–27. [CrossRef]
24. Aiello, G. Submarine Instability Processes on the Continental Slope Offshore of Campania (Southern Italy). *GeoHazards* **2025**, *6*, 20. [CrossRef]
25. Hovland, M.; Judd, A. *Seabed Pockmarks and Seepages: Impact on Geology, Biology and the Marine Environment*; Graham and Trotman Editor: London, UK, 1988. [CrossRef]
26. Aiello, G.; Marsella, E.; Di Fiore, V. New seismo-stratigraphic and marine magnetic data of the Gulf of Pozzuoli (Naples Bay, Tyrrhenian Sea, Italy): Inferences for the tectonic and the magmatic events of the Phlegrean Fields volcanic complex (Campania). *Mar. Geophys. Res.* **2012**, *33*, 97–125. [CrossRef]

27. Aiello, G.; Giordano, L.; Giordano, F. High-resolution seismic stratigraphy of the Gulf of Pozzuoli (Naples Bay) and relationships with submarine volcanic setting of the Phlegrean Fields volcanic complex. *Rend. Lincei Sci. Fis. E Nat.* **2016**, *27*, 775–801. [CrossRef]
28. Kopp, H.; Chiocci, F.L.; Berndt, C.; Çağatay, M.N.; Ferreira, T.; Fortes, C.J.E.M.; Gràcia, E.; González Vega, A.; Kopf, A.J.; Sørensen, M.B.; et al. *Marine Geohazards: Safeguarding Society and the Blue Economy from a Hidden Threat*; Muñiz Piniella, A., Kellett, P., van den Brand, R., Alexander, B., Rodríguez Perez, A., Van Elslander, J., Heymans, J.J., Eds.; Position Paper 26 of the European Marine Board; European Marine Board IVZW: Ostend, Belgium, 2021; p. 100. ISSN 2593-5232. ISBN 9789464206111. [CrossRef]
29. Isaia, R.; Vitale, S.; Di Giuseppe, M.G.; Iannuzzi, E.; D'Assisi Tramparulo, F.; Troiano, A. Stratigraphy, structure, and volcano-tectonic evolution of Solfatara maar-diatreme (Campi Flegrei, Italy). *Geol. Soc. Am. Bull.* **2015**, *127*, 1–20. [CrossRef]
30. Bernardinetti, S.; Bruno, P.P.G. The Hydrothermal System of Solfatara Crater (Campi Flegrei, Italy) Inferred From Machine Learning Algorithms. *Front. Earth Sci.* **2019**, *7*, 286. [CrossRef]
31. Mayer, K.; Scheu, B.; Montanaro, C.; Yilmaz, T.I.; Isaia, R.; Aßbichler, D.; Dingwell, D.B. Hydrothermal alteration of surficial rocks at Solfatara (Campi Flegrei): Petrophysical properties and implications for phreatic eruption processes. *J. Volcanol. Geotherm. Res.* **2016**, *320*, 128–143. [CrossRef]
32. de'Gennaro, M.; Cappelletti, P.; Langella, A.; Perrotta, A.; Scarpati, C. Genesis of zeolites in the Neapolitan Yellow Tuff: Geological, volcanological and mineralogical evidence. *Contrib. Mineral. Petrol.* **2000**, *139*, 17–35. [CrossRef]
33. Isaia, R.; Vitale, S.; Marturano, A.; Aiello, G.; Barra, D.; Ciarcia, S.; Iannuzzi, E.; D'Assisi Tramparulo, F. High-resolution geological investigations to reconstruct the long-term ground movements in the last 15 kyr at Campi Flegrei caldera (southern Italy). *J. Volcanol. Geoth. Res.* **2019**, *385*, 143–158. [CrossRef]
34. Tornero, V.; Ribera d'Alcalà, M. Contamination by hazardous substances in the Gulf of Naples and nearby coastal areas: A review of sources, environmental levels and potential impacts in the MSFD perspective. *Sci. Total Environ.* **2014**, *466–467*, 820–840. [CrossRef] [PubMed]
35. Grezio, A.; Cinti, F.R.; Costa, A.; Faenza, L.; Perfetti, P.; Pierdominici, S.; Pondrelli, S.; Sandri, L.; Tierz, P.; Tonini, R.; et al. Multisource Bayesian probabilistic tsunami hazard analysis for the Gulf of Naples (Italy). *J. Geophys. Res. Oceans* **2020**, *125*, e2019JC015373. [CrossRef]
36. Polonia, A.; Bonatti, E.; Camerlenghi, A.; Lucchi, R.; Panieri, G.; Gasperini, L. Mediterranean megaturbidite triggered by the AD 365 Crete earthquake and tsunami. *Sci. Rep.* **2013**, *3*, 1285. [CrossRef]
37. Mattei, G.; Di Luccio, D.; Benassai, G.; Anfuso, G.; Budillon, G.; Aucelli, P. Characteristics and coastal effects of a destructive marine storm in the Gulf of Naples (southern Italy). *Nat. Hazards Earth Syst. Sci.* **2021**, *21*, 3809–3825. [CrossRef]
38. Aiello, G.; Sacchi, M. New morpho-bathymetric data on marine hazard in the offshore of Gulf of Naples (Southern Italy). *Nat. Hazards* **2022**, *111*, 2881–2908. [CrossRef]
39. Budillon, F.; Martorelli, E.; Conforti, A.; De Falco, G.; Bosman, A.; Di Martino, G.; Firetto Carlino, M.; Misuraca, M.; Innangi, S.; Pierdomenico, M.; et al. Geohazard features of the Gulf of Naples and Pontine Islands (Eastern Tyrrhenian Sea). *J. Maps* **2024**, *20*, 2378935. [CrossRef]
40. Kilburn, C.R.J.; Carlino, S.; Danesi, S.; Pino, N.A. Potential for rupture before eruption at Campi Flegrei caldera, Southern Italy. *Commun. Earth Environ.* **2023**, *4*, 190. [CrossRef]
41. Giudicepietro, F.; Avino, R.; Bellucci Sessa, E.; Bevilacqua, A.; Bonano, M.; Caliro, S.; Casu, F.; De Cesare, W.; De Luca, C.; De Martino, P.; et al. Burst-like swarms in the Campi Flegrei caldera accelerating unrest from 2021 to 2024. *Nat. Commun.* **2025**, *16*, 1548. [CrossRef] [PubMed]
42. Parascandola, A. *I Fenomeni Bradisismici del Serapeo di Pozzuoli*; Guida Editori: Napoli, Italy, 1947; pp. 1–117.
43. Cinque, A.; Russo, M.; Pagano, M. La successione di terreni di età post-romana delle terme di Miseno (Napoli): Nuovi dati per la storia e la stratigrafia del bradisisma puteolano. *Boll. Soc. Geol. Ital.* **1991**, *110*, 231–244.
44. Dvorak, J.J.; Mastrolorenzo, G. *The Mechanisms of Recent Vertical Crustal Movements in Campi Flegrei Caldera, Southern Italy*; Gological Society of America: Boulder, CO, USA, 1991; Volume 263, pp. 1–47.
45. Morhange, C.; Marriner, R.; Laborel, J.; Todesco, M.; Oberlin, C. Rapid sea-level movements and noneruptive crustal deformations in the Phlegrean Fields caldera, Italy. *Geology* **2005**, *34*, 93–96. [CrossRef]
46. Berrino, G.; Corrado, G.; Luongo, G.; Toro, B. Ground deformation and gravity changes accompanying the 1982 Pozzuoli uplift. *Bull. Volcanol.* **1984**, *44*, 187–200. [CrossRef]
47. Vacchi, M.; Marriner, N.; Morhange, C.; Spada, G.; Fontana, A.; Rovere, A. Multiproxy assessment of Holocene relative sea-level changes in the western Mediterranean: Sea-level variability and improvements in the definition of the isostatic signal. *Earth-Sci. Rev.* **2016**, *155*, 172–197. [CrossRef]
48. Astort, A.; Trasatti, E.; Caricchi, L.; De Martino, P.; Acocella, V.; Di Vito, M.A. Tracking the 2007–2023 magma-driven unrest at Campi Flegrei caldera (Italy). *Commun. Earth Environ.* **2024**, *5*, 506. [CrossRef]
49. Patanè, D.; Barberi, G.; Martino, C. Seismic Images of Pressurized Sources and Fluid Migration Driving Uplift at the Campi Flegrei Caldera During 2020–2024. *GeoHazards* **2025**, *6*, 19. [CrossRef]

50. Rosi, M.; Sbrana, A. *Phlegrean Fields*; Quaderni De La Ricerca Scientifica; Consiglio Nazionale Delle Ricerche (CNR) Italiano: Roma, Italy, 1987; Volume 114, pp. 1–175.
51. Di Vito, M.A.; Isaia, R.; Orsi, G.; Southon, J.; De Vita, S.; D'Antonio, M.; Pappalardo, L.; Piochi, M. Volcanism and deformation since 12,000 years at the Campi Flegrei caldera (Italy). *J. Volcanol. Geoth. Res.* **1999**, *91*, 221–246. [CrossRef]
52. Nunziata, C.; Mele, R. Natale, M Shear wave velocities and primary influencing factors of Campi Flegrei—Neapolitan deposits. *Engineer. Geol.* **1999**, *54*, 299–312. [CrossRef]
53. Orsi, G.; De Vita, S.; Di Vito, M.A.; Isaia, R.; Nave, R.; Heiken, G. Facing volcanic and related hazard in the Neapolitain area. In *Earth Sciences in the City*; Heiken, G., Fakundiny, R., Sutter, J., Eds.; American Geophysical Union Special Publication: Washington, DC, USA, 2002; pp. 121–170.
54. Orsi, G.; Di Vito, M.A.; Selva, J.; Marzocchi, W. Long-term forecast of eruption style and size at Campi Flegrei caldera (Italy). *Earth Planet. Sci. Lett.* **2009**, *287*, 265–276. [CrossRef]
55. D'Argenio, B.; Aiello, G.; de Alteriis, G.; Milia, A.; Sacchi, M.; Tonielli, R.; Budillon, F.; Chiocci, F.L.; Conforti, A.; De Lauro, M.; et al. *Digital Elevation Model of the Naples Bay and Adjacent Areas, Eastern Tyrrhenian Sea*; Atlante di Cartografia Geologica scala 1:50,000 (progetto CARG); 32° International Congress "Firenze 2004"; Servizio Geologico d'Italia (APAT): Firenze, Italy; Editore De Agostini: Novara, Italy, 2004.
56. Deino, A.L.; Orsi, G.; Piochi, M.; de Vita, S. The age of the Neapolitan Yellow Tuff caldera-forming eruption (Campi Flegrei caldera—Italy) assessed by 40Ar/39Ar dating method. *J. Volcanol. Geoth. Res.* **2004**, *133*, 157–170. [CrossRef]
57. Milia, A.; Torrente, M.M. The influence of paleogeographic setting and crustal subsidence on the architecture of ignimbrites in the Bay of Naples (Italy). *Earth Plan. Sci. Lett.* **2007**, *263*, 192–206. [CrossRef]
58. Blockley, S.P.E.; Ramsey, C.B.; Pyle, D.M. Improved age modeling and high-precision age estimates of late Quaternary tephras, for accurate paleoclimate reconstruction. *J. Volcanol. Geoth. Res.* **2008**, *177*, 251–262. [CrossRef]
59. Sacchi, M.; Pepe, F.; Corradino, M.; Insinga, D.D.; Molisso, F.; Lubritto, C. The Neapolitan Yellow Tuff caldera offshore the Campi Flegrei: Stratal architecture and kinematic reconstruction during the last 15 ky. *Mar. Geol.* **2014**, *354*, 15–33. [CrossRef]
60. Steinmann, L.; Spiess, V.; Sacchi, M. The Campi Flegrei caldera (Italy): Formation and evolution in interplay with sea-level variations since the Campanian Ignimbrite eruption at 39 ka. *J. Volcanol. Geoth. Res.* **2016**, *327*, 361–374. [CrossRef]
61. Steinmann, L.; Spiess, V.; Sacchi, M. Post-collapse evolution of a coastal caldera system: Insights from a 3D multichannel seismic survey from the Campi Flegrei caldera (Italy). *J. Volcanol. Geoth. Res.* **2018**, *349*, 83–98. [CrossRef]
62. Barberi, F.; Innocenti, F.; Lirer, L.; Munno, R.; Pescatore, T.S.; Santacroce, R. The Campanian Ignimbrite: A major prehistoric eruption in the Neapolitan area (Italy). *Bull. Volcanol.* **1978**, *41*, 10–27. [CrossRef]
63. Rolandi, G.; Bellucci, F.; Heizler, M.T.; Belkin, H.E.; De Vivo, B. Tectonic controls on the genesis of ignimbrites from the Campanian Volcanic Zone, southern Italy. *Mineral. Petrol.* **2003**, *79*, 3–31. [CrossRef]
64. Marianelli, P.; Sbrana, A.; Proto, M. Magma chamber of the Campi Flegrei supervolcano at the time of eruption of the Campanian Ignimbrite. *Geology* **2006**, *34*, 937–940. [CrossRef]
65. Pyle, D.M.; Ricketts, G.D.; Margari, V.; van Andel, T.H.; Sinitsyn, A.A.; Praslov, N.D.; Lisitsyn, S. Wide dispersal and deposition of distal tephra during the Pleistocene 'Campanian Ignimbrite/Y5' eruption, Italy. *Quat. Sci. Rev.* **2006**, *25*, 2713–2728. [CrossRef]
66. Fitzsimmons, K.E.; Hambach, U.; Veres, D.; Iovita, R. The Campanian Ignimbrite Eruption: New Data on Volcanic Ash Dispersal and Its Potential Impact on Human Evolution. *PLoS ONE* **2013**, *8*, e65839. [CrossRef]
67. Forni, F.; Bachmann, O.; Mollo, S.; De Astis, G.; Gelman, S.E.; Ellis, B.S. The origin of a zoned ignimbrite: Insights into the Campanian Ignimbrite magma chamber (Campi Flegrei, Italy). *Earth Plan. Sci. Lett.* **2016**, *449*, 259–271. [CrossRef]
68. Marti, A.; Folch, A.; Costa, A.; Engwell, S. Reconstructing the plinian and co-ignimbrite sources of large volcanic eruptions: A novel approach for the Campanian Ignimbrite. *Sci. Rep.* **2016**, *6*, 21220. [CrossRef]
69. Scarpati, C.; Sparice, D.; Perrotta, A. Comparative proximal features of the main Plinian deposits (Campanian Ignimbrite and Pomici di Base) of Campi Flegrei and Vesuvius. *J. Volcanol. Geotherm. Res.* **2016**, *321*, 149–157. [CrossRef]
70. Giaccio, B.; Hajdas, I.; Isaia, R.; Deino, A.; Nomade, S. High-precision ^{14}C and ^{40}Ar/^{39}Ar dating of the Campanian Ignimbrite (Y-5) reconciles the timescales of climatic-cultural processes at 40 ka. *Sci. Rep.* **2017**, *7*, 45940. [CrossRef]
71. Silleni, A.; Giordano, G.; Isaia, R.; Ort, M.H. The Magnitude of the 39.8 ka Campanian Ignimbrite Eruption, Italy: Method, Uncertainties and Errors. *Front. Earth Sci.* **2020**, *8*, 543399. [CrossRef]
72. Rolandi, G.; Di Lascio, M.; Rolandi, R. 11—The Neapolitan Yellow Tuff eruption as the source of the Campi Flegrei caldera. In *Vesuvius, Campi Flegrei and Campanian Volcanism*; De Vivo, B., Harvey, E., Belkin, H.E., Rolandi, G., Eds.; Elsevier: Amsterdam, The Netherlands, 2020; pp. 273–296. [CrossRef]
73. Vineberg, S.O.; Isaia, R.; Albert, P.G.; Brown, R.J.; Smith, V.C. Insights into the explosive eruption history of the Campanian volcanoes prior to the Campanian Ignimbrite eruption. *J. Volcanol. Geoth. Res.* **2023**, *443*, 107915. [CrossRef]
74. Sbrana, A.; Marianelli, P.; Pasquini, G. The Phlegrean Fields volcanological evolution. *J. Maps* **2021**, *17*, 557–570. [CrossRef]

75. Natale, J.; Ferranti, L.; Marino, C.; Sacchi, M. Resurgent dome faults in the offshore of the Campi Flegrei caldera (Pozzuoli Bay, Campania): Preliminary results from high-resolution seismic reflection profiles. *Boll. Di Geofis. Teor. Appl.* **2020**, *61*, 333–342. [CrossRef]
76. Vitale, S.; Isaia, R. Fractures and faults in volcanic rocks (Campi Flegrei, southern Italy): Insight into volcano-tectonic processes. *Int. J. Earth Sci. (Geol. Rundsch.)* **2014**, *103*, 801–819. [CrossRef]
77. Vitale, S.; Isaia, R.; Ciarcia, S.; Di Giuseppe, M.G.; Iannuzzi, E.; Prinzi, E.P.; Tramparulo, F.D.A.; Troiano, A. Seismically induced soft-sediment deformation phenomena during the volcano-tectonic activity of Campi Flegrei caldera (southern Italy) in the last 15 kyr. *Tectonics* **2019**, *38*, 1999–2018. [CrossRef]
78. Natale, J.; Camanni, G.; Ferranti, L.; Isaia, R.; Sacchi, M.; Spiess, V.; Steinmann, L.; Vitale, S. Fault systems in the offshore sector of the Campi Flegrei caldera (southern Italy): Implications for nested caldera structure, resurgent dome, and volcano-tectonic evolution. *J. Struct. Geol.* **2022**, *163*, 104723. [CrossRef]
79. Orsi, G.; De Vita, S.; Di Vito, M. The restless, resurgent Campi Flegrei nested caldera (Italy): Constraints on its evolution and configuration. *J. Volcanol. Geotherm. Res.* **1996**, *74*, 179–214. [CrossRef]
80. Turner, R.; Ahmed, M.; Bissell, R.; Prothro, L.O.; Shehata, A.A.; Coffin, R. Structural and stratigraphic controls on reservoir architecture: A case study from the lower Oligocene Vicksburg Formation, Brooks County, Texas. *Mar. Pet. Geol.* **2024**, *160*, 106627. [CrossRef]